Cerebral Cortex Advance Access published August 6, 2014

Cerebral Cortex
doi:10.1093/cercor/bhu168

Neural Anatomy of Primary Visual Cortex Limits Visual Working Memory

Johanna Bergmann[1,2,3], Erhan Genç[2,3,4], Axel Kohler[2,3,5], Wolf Singer[2,3,6,7] and Joel Pearson[1]

[1]School of Psychology, University of New South Wales, 2052 Sydney, Australia, [2]Department of Neurophysiology, Max-Planck-Institute for Brain Research, 60528 Frankfurt am Main, Germany, [3]Brain Imaging Center Frankfurt, 60528 Frankfurt am Main, Germany, [4]Institute of Psychology, Biopsychology, Ruhr-University Bochum, 44780 Bochum, Germany, [5]Institute of Cognitive Science, University of Osnabrück, 49076 Osnabrück, Germany, [6]Frankfurt Institute for Advanced Studies, Goethe University, 60438 Frankfurt am Main, Germany and [7]Ernst Strüngmann Institute in Cooperation with Max Planck Society, 60528 Frankfurt am Main, Germany

Address correspondence to Joel Pearson. Email: joel@pearsonlab.org

Despite the immense processing power of the human brain, working memory storage is severely limited, and the neuroanatomical basis of these limitations has remained elusive. Here, we show that the stable storage limits of visual working memory for over 9 s are bound by the precise gray matter volume of primary visual cortex (V1), defined by fMRI retinotopic mapping. Individuals with a bigger V1 tended to have greater visual working memory storage. This relationship was present independently for both surface size and thickness of V1 but absent in V2, V3 and for non-visual working memory measures. Additional whole-brain analyses confirmed the specificity of the relationship to V1. Our findings indicate that the size of primary visual cortex plays a critical role in limiting what we can hold in mind, acting like a gatekeeper in constraining the richness of working mental function.

Keywords: cortical thickness, early visual cortex, gray matter surface size, individual differences, visual working memory

Introduction

Visual working memory is necessary to actively maintain representations of a visual scene once it has gone, thereby providing an essential link between sensory processing and higher cognitive functions (Baddeley 2003). Yet, the ability to temporarily store visual information is severely limited and subject to large inter-individual variation, the neurophysiological underpinnings of which have so far remained unclear.

Opposing theory and data regarding both the capacity limits and neural correlates of visual working memory have led to much debate in recent years. Such discussions have evolved around neural activity in high-level areas (Pessoa et al. 2002; Todd and Marois 2004; Xu and Chun 2005; Serences et al. 2009), but a growing body of newer evidence also suggests that early visual areas (V1–V3) may play a vital role in working memory by maintaining information about specific features of an item, such as spatial orientation (Harrison and Tong 2009; Serences et al. 2009; Riggall and Postle 2012; Emrich et al. 2013; Ester et al. 2013) or contrast (Xing et al. 2013).

Research on individual differences in visual working memory has found some indications for an influence of neural activity in higher-level areas (Vogel and Machizawa 2004; Todd and Marois 2005). However, there is good reason to assume that these differences might also be strongly influenced by properties of early sensory areas, in particular primary visual cortex (V1). The neural anatomy of this retinotopically organized area varies greatly inter-individually, with V1 surface size varying by a factor of 3–4 between individuals (Filimonov 1932; Stensaas et al. 1974). Recent work in the field of visual perception has been able to link this variability in the structural organization of V1 to differences in conscious experience. For example, while visual acuity can be predicted by the size of the allocated cortical surface in V1 within an individual (Duncan and Boynton 2003), inter-individual variation in the surface size of V1 has been associated with differences in visual illusion strength (Schwarzkopf et al. 2011; Schwarzkopf and Rees 2013), the speed of binocular rivalry-induced perceptual waves (Genç et al. 2014), and spatial orientation sensitivity (Song et al. 2013). Given that early visual cortex is not only essential for perceptual processing, but also important for retaining more finely tuned visual information about a stimulus during memory processing, it seems likely that the large neuroanatomical differences might not only have an impact on individual differences in perception but also shape the characteristics of visual working memory storage. This idea is particularly intriguing as a recent model of visual working memory proposes that storage limits are set by two-dimensional visual "map" representations, such that individual items would compete for neuroanatomical "real estate" (Franconeri et al. 2013). Accordingly, the degree to which memory items (and also parts of an item, if it is remembered at a higher precision) interfere with each other, and hence the number of items that can be remembered, depends on the size of the representations in the map, the distance between the items, and the extent of surround inhibition of each item. Following the rationale of this model, one should expect the representational visual map to be larger in individuals with a larger V1 surface. This could have 2 consequences: First, the space allocated to representing the individual patterns on the map would be larger. Second, the distance between the items would be increased, resulting in less inter-item interference and hence a higher number of items that can be held in memory.

The aim of the current study was to investigate the relationship between individual variability in behavior and brain anatomy using a combined approach of behavioral testing and fMRI retinotopic mapping. We found that while perceptual encoding of the stimuli was near perfect, the individual differences in visual working memory storage were indeed predicted by the anatomical measures of V1 volume, surface size, and cortical thickness. Both the anatomical and the behavioral measures showed good reliability, and there was no correlation with the anatomy of other brain regions or between V1 anatomy and numerical working memory (NWM) storage.

Materials and Methods

Participants

Thirty-one right-handed participants, ages ranging from 18 to 36 (median: 26; 13 males), took part in the study. The number working memory task was tested on a subsample of the original sample ($N = 17$, age range: 18–36; 8 males), and a perceptual/iconic version of the visual working memory task was tested in another subsample of $N = 13$ (age range: 18–36; 8 males). None of the participants had any history of psychiatric or neurological disorders. All participants had normal or corrected-to-normal vision and were paid for participation. Written informed consent was obtained from all participants, and the study was approved by the ethics committee of the Max Planck Society.

Behavioral Experiments

Apparatus

Stimuli in the behavioral tasks were presented on a CRT monitor (HP p1230; resolution, 1024 × 768 pixels) at a refresh rate of 150 Hz and controlled by MATLAB R2010a (The MathWorks) using the Psychophysics Toolbox extension (Brainard 1996; Pelli 1997; Kleiner et al. 2007), running on Mac OSX, version 10.7.4. Observers sat in a darkened room at a distance of 75 cm to the screen, their position fixed with a chin rest. The visible screen size was 30° × 22.9°.

Stimuli

In the visual working memory task, 2–4 Gabor patterns were used as stimuli in front of an otherwise black background. They surrounded the fixation point in a circular fashion at an eccentricity of 6.4° in visual angle. The stimuli were circularly shaped, with a diameter 1.8°, so that their outer boundary was at a distance of 7.2° to the fixation point, and the inner boundary at a distance of 5.5°. One period subtended a length of 0.8°. Each of the Gabor gratings had a unique orientation, and this orientation was randomly varied with each trial. The background remained black (<0.1 cd/m^2), whereas the stimuli were white (peak luminance in the center of the stimuli: 9.0 cd/m^2).

In the number working memory task, which was used as a control task and tested on a smaller subsample of the participants, 5–8 white numbers were presented (5–7 in 2 of the participants) on a black background, surrounding the fixation point in a circular fashion at the same distance from fixation as the Gabor patterns in the visual working memory task. Analogously, their sizes matched that of the Gabor stimuli, and their luminance was approximately the mean of the luminance of the Gabor stimuli (which were brighter in the center and faded toward the outer boundaries). The numbers were randomized in each trial, with no 2 identical numbers placed next to each other.

Procedure

Behavioral tests took place in 2 sessions, with an interval of 1–4 weeks in between (~2 weeks on average). The number working memory task, which was tested on a subsample of the original sample, was tested in another separate session. In addition, standard fMRI retinotopic-mapping scans of all participants were acquired in a different session (see further below).

Visual Working Memory. The task procedure is illustrated in Figure 1. In each trial, participants held fixation while presented with an array of differently and randomly oriented Gabor patches for 1 s. The patches were presented in the periphery, surrounding the fixation point circularly, as described earlier. The set size varied randomly between 2 and 4 patches in every trial, with an equal number of each. After an inter-stimulus interval of 9.3 s, another Gabor patch was presented, at a random location where one of the previous array patches had been. In comparison to the previous Gabor pattern, the orientation of the "new" Gabor was rotated by 20°, clockwise or anticlockwise. Participants were required to indicate whether the patch had been rotated clockwise or anticlockwise by pressing either the right or left arrow key (two-alternative forced choice, 2AFC). The patch stayed on the screen until the participant gave the response. In each of the 2 test sessions, participants completed a total of 36 trials, 12 per array size (thus, 24 over the 2 sessions in total). In a variation of the task to measure "perceptual encoding" of the visual stimuli, which was tested in a subsample of the participants ($N = 13$), the inter-stimulus interval was reduced to 120 ms whereas all other settings remained the same.

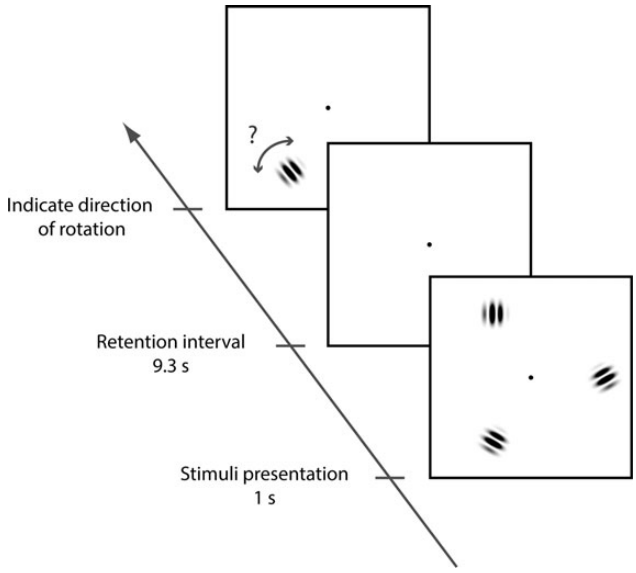

Figure 1. Behavioral task. In the visual working memory task, participants were first presented a circular array of Gabor stimuli on a black background for 1 s and asked to memorize their orientations (colors are inverted here for better visibility). After a retention interval of 9.3 s, a new Gabor stimulus appeared randomly at 1 of the locations where the stimuli had been presented. By pressing 1 of 2 buttons, participants indicated the direction in which the new stimulus had been rotated compared with the previous one (in this figure, the correct response would be "clockwise").

Number Working Memory. In this task, the timing was the same as in the visual working memory task. However, instead of the Gabor stimuli, a varying number of 5–8 numbers were presented in a circular fashion around the fixation point, at the same eccentricity as the Gabor gratings in the visual working memory task. Following the test array and the ISI, 2 circular arrays of numbers were presented again, each one shown for 2 s, with a 1-s interval in between. One of these number arrays was identical to the test array, whereas in the other array, one of the numbers, which was randomly selected in each trial, was different. Participants were then asked to indicate which of the 2 arrays was completely identical to the test array by pressing 1 of 2 keys. Participants completed a set of 96 trials in 1 session (no retest session), 24 per number length. In 2 participants, only set sizes 5–7 were measured; in another participant, we had a dataset of only 12 trials in the 8 stimuli condition.

Analysis of Behavioral Data

Correlation and regression analyses were computed in PASW Statistics, version 22.0.0. Cowan's K, and 75%-quantiles from linear curve fits were computed in MATLAB R2010a (The MathWorks). Hotelling's T was computed using the FZT Computator (http://psych.unl.edu/psycrs/statpage/regression.html). Cowan's K is a measure typically applied in Change/No Change paradigms that are often used in VWM tasks. As the probe stimulus in our task had always been rotated (either clockwise or anticlockwise in comparison to the test stimulus), we were required to arbitrarily assign 1 condition ("clockwise rotation" of the probe) as the "change" condition, and the other condition ("anticlockwise rotation") as the "no change" condition to compute it. We analyzed our data using Cowan's K accordingly using the formula $K = S \times (H - F)$, where K is the memory capacity, S is the size of the array, H is the observed hit rate, and F is the false alarm rate (Vogel and

Machizawa 2004). We then estimated individual VWM using the average of each session's peak of Cowan's *K*, that is, each individual's maximal *K* value across set sizes.

MRI Measurement

The neuroimaging and data analysis procedure to obtain retinotopic maps from our individuals matched those already described in Genç et al. (2014).

Acquisition of Imaging Data

All neuroimaging measurements were done at the Brain Imaging Center Frankfurt am Main, Germany, in a Siemens 3-Tesla Trio (Siemens) with an 8-channel head coil and a maximum gradient strength of 40 mT/m.

Structural MRI Data. T1-weighted high-resolution anatomical images were acquired from all participants for reasons of co-registration and anatomical localization of the functional data (MP-RAGE, TR = 2250 ms, TE = 2.6 ms, flip angle: 9°, FoV: 256 mm, voxel size = 1 × 1 × 1 mm^3).

Functional MRI Data. For the retinotopic-mapping measurements, a gradient-recalled echo-planar-imaging sequence was applied (33 slices, TR = 2000 ms, TE = 30 ms, flip angle = 90°, FoV = 192 mm, slice thickness = 3 mm, gap thickness = 0.3 mm, voxel size = 3.0 × 3.0 × 3.0 mm^3). Our stimuli were generated with a custom-made program based on the Microsoft DirectX library (Muckli et al. 2005) and presented using an MR-compatible goggle system with 2 organic light-emitting-diode displays (MR Vision 2000; Resonance Technology). The maximal visual field subtended a visual angle of 24° vertically and 30° horizontally.

Stimuli for Retinotopic Mapping

To obtain retinotopic maps of the early visual areas, participants underwent functional MRI scanning while viewing rotating wedge and expanding ring stimuli. By inducing spatial sequences of neural activity in the visual cortex through phase-encoded retinal stimulation, this method allowed us to determine the borders between adjacent early visual areas and their anterior expansion along the medial wall of the occipital cortex (Sereno et al. 1995; Wandell et al. 2007). To map the polar angle, which allowed us to determine the borders between adjacent visual areas, participants were presented a wedge-shaped black and white checkerboard pattern that slowly rotated around the fixation point. The wedge stimulus subtended a visual angle of 22.5° and extended to 15° in the periphery from the central fixation point. The background was gray. The wedge started at the 3 o'clock position (the right horizontal meridian) and rotated clockwise around the fixation point 12 times for a full circle of 360° at a speed of 11.25° in polar angle/volume (2 s), each cycle lasting 64 s. In the eccentricity-mapping experiment, a slowly expanding ring-shaped checkerboard pattern was presented. The resulting phase-encoded neural activity of this stimulation allowed us to determine radii of eccentricity on the surface of the visual areas that match visual angles from the center of gaze in vision. Reversing the contrast at a flickering rate of 4 Hz, the ring started with a radius of 1° and slowly increased to a radius of 15°. The measurement consisted of 7 of these expansion cycles, each lasting 64 s. During both measurements, participants were instructed to fixate on the central fixation point.

Analysis of Imaging Data

FreeSurfer and FSFAST were used to reconstruct the cortical surfaces and perform the analyses of the functional data (http://surfer.nmr.mgh.harvard.edu, version 5.1.0).

Anatomical Data. Surface-based methods as implemented in the FreeSurfer environment were used to reconstruct the cortical surface from the T1-weighted image (http://surfer.nmr.mgh.harvard.edu/fswiki/RecommendedReconstruction); the reconstruction steps included Talairach transformation, skull stripping, white and gray matter segmentation, reconstruction and inflation of the cortical surface (Dale et al. 1999; Fischl, Sereno and Dale 1999). Note that only the Talairach *transformation* is computed, but the *volume* itself is not resampled to Talairach space, so the anatomical measures are not affected by warping (see http://ftp.nmr.mgh.harvard.edu/fswiki/FsTutorial/MorphAndRecon). These processing steps were performed for each participant individually. Where necessary, the automatic steps were corrected manually.

Functional Data. FSFAST was used to process the functional data of the retinotopic polarity and eccentricity mapping. Preprocessing steps included slice-time correction, motion correction and co-registration to the T1-weighted anatomical images. For each voxel, a Fourier transform was applied to extract the amplitude and phase at stimulation frequency, which was 12 cycles/run in the polarity mapping and 7 cycles/run in the eccentricity mapping. The phase of the periodic response at stimulation frequency is linked to the polar angle or eccentricity that is represented at the cortical location of the voxel. Then, phase angles were mapped to different colors, where each color represents a response phase whose intensity is an F-ratio between the squared amplitude of the response at the stimulus frequency with the average squared amplitudes at all other frequencies (higher harmonics of the stimulus frequency and low-frequency signals were excluded). The resulting polarity and eccentricity phase maps that were computed separately for each participant were displayed on the reconstructed inflated cortical surface of the participant's T1-weighted image. The boundaries of V1, V2 and V3 were then delineated manually and individually for each participant on the basis of phase-encoded retinotopy. Using FreeSurfer's Anatomical ROI analysis tool, we then determined the early visual areas' volume, surface size and mean cortical thickness values up to an eccentricity of 7.2° from the center of gaze, which matches the outer visual angle at which the Gabor patches were presented in the visual working memory task. As a control in the multiple regression analyses (see Results) and in bivariate correlations (see Supplementary Material), we also computed each individual's overall brain volume, surface size, and average cortical thickness.

The manual estimation of the early visual cortex boundaries was done by 2 independent raters, the first and second author, who were blind to each other's mappings. This was done before the behavioral data were processed and analyzed, so both raters were unaware of the participants' performance to prevent potential biases in their judgments. When correlating the delineations of both raters with each other, the inter-rater reliability showed a very strong concordance between the 2 ratings for V1 and V2 volume (V1: $r = 0.913$, $P < 0.001$; V2: $r = 0.901$, $P < 0.001$). In V3, the agreement between the 2 raters was slightly lower ($r = 0.631$, $P < 0.001$).

When distinguishing between surface size and cortical thickness, the agreement between the raters followed a similar pattern: Inter-rater reliability showed a very strong concordance between the 2 ratings for V1 surface and thickness (V1 surface: $r = 0.900$, $P < 0.001$; V1 thickness: $r = 0.970$, $P < 0.001$) and V2 surface and thickness (V2 surface: $r = 0.908$, $P < 0.001$; V2 thickness: $r = 0.965$, $P < 0.001$). In V3, the agreement between the 2 raters was slightly lower for surface ($r = 0.634$, $P < 0.001$) but remained very high for thickness ($r = 0.946$, $P < 0.001$).

For computing the relationships with behavior, the average of the volume, surface and thickness ratings of the 2 raters were used.

Anatomical Parcellation of V1. Apart from estimating the boundaries of early visual cortex functionally, we used Freesurfer's surface-based probabilistic method to predict V1 boundaries in each participant individually (Hinds et al. 2008). Functional mapping covers large parts of V1 due to cortical magnification, which means that the cortical representation of the central visual field is much larger compared with that of the visual periphery. Nevertheless, a potentially substantial amount of V1 might be left out. The surface-based prediction method based on anatomical landmarks instead aims to measure the area of V1 in its entirety. To reduce bias, a highly conservative threshold of 0.8 was used, which is the probability that the actual boundary of V1 lies within the predicted boundary. Again, volume, surface, and thickness of the defined areas were determined and related to behavior.

Cortical Thickness Analysis of the Whole Cortex. In addition to determining cortical thickness of the functionally defined early visual areas, we used the surface-based analysis approach to derive morphometric measures of the whole brain using FreeSurfer's Qdec application. After having preprocessed the anatomical data as described earlier, the surface, thickness, and curvature data of each participant were smoothed using a full width at half-maximum Gaussian filter of 10 mm. Then, group alignment was achieved in a surface-based spatial normalization step, where each individual surface was first transformed into a spherical representation and then non-rigidly adjusted to a common-space spherical surface (fsaverage) so to best match the folding patterns (Fischl, Sereno, Tootell et al. 1999). After this step, thickness data of each participant were applied to the common group space, which allowed for cortical thickness comparisons across participants at homologous points within the brain. Vertex-wise correlations with the behavioral parameters were computed, and results were tested using a pre-cached Monte Carlo Null-Z simulation with 10 000 iterations and a cluster-wise probability threshold of $P < 0.05$ to correct for multiple comparisons (Hagler et al. 2006).

Results

Between-subject variability in the size of early visual cortex was substantial, and the blind inter-rater reliability of the functionally defined regions was very high (see Materials and Methods). The 2-week retest-reliability of VWM was highest for set size 3 ($r = 0.671$, $P < 0.001$; see Supplementary Fig. S1), with inter-individual variability ranging from 54.17% to 100% correct. Retest reliability at the other 2 set sizes was lower, presumably due to the ceiling effect at set size 2, which strongly reduced inter-individual variability, and possibly due to inconsistencies in the applied strategy and clustering issues in set size 4 (see Supplementary Results and Supplementary Fig. S1). We therefore focus on percent correct at set size 3 as the primary measure of VWM storage, as this set size appears to be large enough to reveal stable and sizable inter-individual differences, while at the same time avoiding the problems that affected the measurements at the other set sizes. However, the relationships between anatomy and behavior also held when other indicators of VWM storage were used, despite their lower retest reliabilities (percent correct at set size 4, Cowan's K and the 75% quantile, which combines data from all set sizes; see Table 1 and Supplementary Results). For set size 2, there were no significant relationships with early visual cortex anatomy (all $P > 0.223$), presumably due to the strongly reduced inter-individual variance.

We found strong positive correlations between VWM (percent correct at set size 3) and V1 volume ($r = 0.563$, $P = 0.001$; see Fig. 2*A*). In contrast, correlations with V2 and V3 as well as with the total brain volume were non-significant (V2: $r = 0.206$, $P = 0.267$, V3: $r = 0.087$, $P = 0.641$, whole brain: $r = 0.228$, $P = 0.218$; see Fig. 2*A*). A multiple linear regression including V1, V2, V3, and total brain volume, age, and gender as independent variables and VWM storage as the dependent variable further confirmed the specificity of the observed relationship. Only V1 volume provided a unique contribution in predicting memory storage (V1 volume: beta = 0.653, $t_{(30)} = 3.361$, $P = 0.003$), whereas the other factors remained non-significant (all $P > 0.319$). This specificity was confirmed in tests for the difference between pairs of correlation values, where the relationship between VWM and V1 volume was significantly stronger than the relationships between VWM and V2/V3 volume (see Supplementary Results).

To take a closer look at the sub-components of gray matter volume, we then examined cortical thickness and surface size separately. Consistent with previous research stating that they are genetically independent (Panizzon et al. 2009; Winkler et al. 2010), we found no correlation between V1 thickness and surface size ($r = -0.094$, $P = 0.614$). However, both were significantly related to VWM, indicating that both serve as independent predictors of the behavior (V1 surface: $r = 0.424$, $P = 0.017$; V1 thickness: $r = 0.512$, $P = 0.003$; see Fig. 2*B*). In an additional multiple linear regression analysis now including both surface size and cortical thickness of V1, V2, V3, and the whole brain, age, and gender as independent variables and VWM storage as the dependent variable, we confirmed that both V1 surface size and V1 thickness provided unique contributions to the prediction of behavior (V1 surface size: beta = 0.513, $t_{(30)} = 2.866$, $P = 0.01$, V1 thickness: beta = 0.651, $t_{(30)} = 3.53$, $P = 0.002$). All other factors remained non-significant (all $P > 0.083$).

Individuals with a larger and/or thicker V1 thus tended to have higher VWM storage (see Fig. 2*B*,*C*). To exclude the possibility that the observed differences in VWM resulted from

Table 1
Statistical relationships between measures of visual working memory, number working memory and early visual cortex anatomy

	Visual working memory				Number working memory
	Set size 3, percent correct	Set size 4, percent correct	Cowan's *K*	75% quantile	75% quantile
Test reliability	**0.671 (*P* < 0.001)**	0.215 (*P* = 0.245)	0.149 (*P* = 0.425)	**0.573 (*P* = 0.003, *N* = 25)**	**0.721 (*P* = 0.004, *N* = 17)**
V1 volume	**0.563 (*P* = 0.001)**	**0.614 (*P* < 0.001)**	**0.551 (*P* = 0.001)**	**0.534 (*P* = 0.002)**	0.148 (*P* = 0.571)
V1 surface size	**0.424 (*P* = 0.017)**	**0.635 (*P* < 0.001)**	**0.477 (*P* = 0.007)**	**0.418 (*P* = 0.019)**	0.086 (*P* = 0.742)
V1 cortical thickness	**0.512 (*P* = 0.003)**	−0.105 (*P* = 0.575)	0.198 (*P* = 0.287)	0.308 (*P* = 0.092)	−0.041 (*P* = 0.876)
V2 volume	0.206 (*P* = 0.267)	0.331 (*P* = 0.069)	0.167 (*P* = 0.370)	0.096 (*P* = 0.606)	0.077 (*P* = 0.769)
V2 surface size	0.045 (*P* = 0.809)	**0.388 (*P* = 0.031)**	0.145 (*P* = 0.437)	0.094 (*P* = 0.616)	0.116 (*P* = 0.657)
V2 cortical thickness	**0.457 (*P* = 0.010)**	−0.016 (*P* = 0.933)	0.187 (*P* = 0.315)	0.042 (*P* = 0.824)	0.057 (*P* = 0.829)
V3 volume	0.087 (*P* = 0.641)	0.134 (*P* = 0.471)	0.028 (*P* = 0.882)	−0.055 (*P* = 0.769)	−0.150 (*P* = 0.566)
V3 surface size	−0.055 (*P* = 0.768)	0.133 (*P* = 0.475)	0.002 (*P* = 0.992)	−0.063 (*P* = 0.737)	−0.236 (*P* = 0.361)
V3 cortical thickness	0.274 (*P* = 0.135)	−0.126 (*P* = 0.499)	−0.047 (*P* = 0.803)	−0.110 (*P* = 0.557)	0.206 (*P* = 0.427)
aV1 volume	**0.439 (*P* = 0.014)**	**0.359 (*P* = 0.047)**	0.292 (*P* = 0.110)	0.270 (*P* = 0.142)	−0.087 (*P* = 0.740)
aV1 surface size	0.157 (*P* = 0.400)	0.215 (*P* = 0.246)	0.050 (*P* = 0.791)	0.038 (*P* = 0.840)	−0.058 (*P* = 0.825)
aV1 cortical thickness	**0.696 (*P* < 0.001)**	0.283 (*P* = 0.123)	**0.448 (*P* = 0.011)**	**0.457 (*P* = 0.010)**	0.084 (*P* = 0.749)
Whole-brain volume	0.228 (*P* = 0.218)	0.011 (*P* = 0.952)	−0.008 (*P* = 0.967)	−0.020 (*P* = 0.916)	−0.088 (*P* = 0.737)
Whole-brain surface size	0.183 (*P* = 0.326)	0.112 (*P* = 0.550)	0.047 (*P* = 0.802)	0.056 (*P* = 0.765)	−0.180 (*P* = 0.490)
Whole-brain cortical thickness	0.170 (*P* = 0.359)	−0.199 (*P* = 0.284)	−0.102 (*P* = 0.584)	−0.163 (*P* = 0.380)	0.194 (*P* = 0.455)

Note: The values indicate bivariate correlations, the *P*-values in brackets their respective significance levels. Significant correlations are written in bold. aV1, anatomically estimated V1 (Hinds et al. 2008).

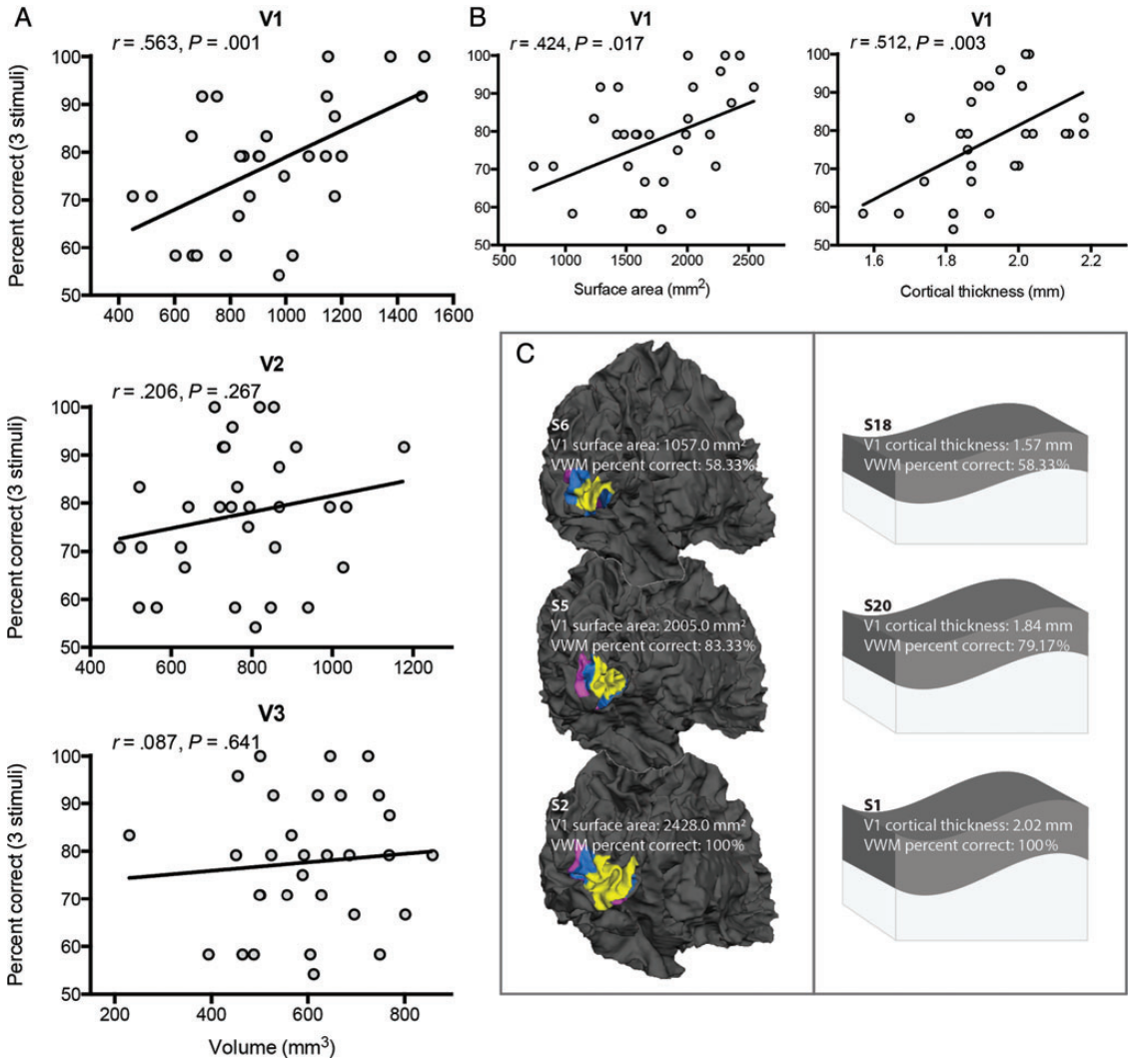

Figure 2. Visual working memory storage is predicted by anatomical properties of V1. (*A*) The scatterplots to the left show the correlation between VWM storage and gray matter volume of early visual cortex. Pearson product-moment correlation coefficients and significance levels are written above each plot. Each data point represents the values of 1 participant in the study whereas the lines delineate the linear regression estimates. We found a significant correlation between V1 and VWM storage, whereas the relationships with V2 (middle) and V3 (bottom) remained non-significant. (*B*) When examining the relationships between behavior and the V1 gray matter components cortical thickness (left) and surface size (right) separately, we found that both predict visual working memory independently (see Supplementary Fig. S5 for the correlations between VWM and V2 and V3 surface size and cortical thickness). (*C*) Left: Early visual cortex surface sizes of 3 participants in our study and their respective VWM scores (only the reconstructed meshes of the left hemispheres are shown). Individuals with a larger surface of V1 (yellow) tended to have a larger VWM storage. However, VWM did not show significant relationships with the size of V2 (blue) and V3 (pink). Right: Graphical illustration depicting gray matter cortical thickness of V1 of 3 participants and their respective VWM scores. Participants with a thicker V1 tended to have a greater VWM storage.

differences at the perceptual encoding stage, we ran another behavioral control experiment on a subsample of our participants ($N = 13$) using the same experimental paradigm as in the VWM task with the difference that the inter-stimulus interval was now reduced to 120 ms. Despite the fact that the individuals in the subsample showed strong individual differences in VWM (subsample performance ranged from 58.33% to 100% correct responses at set size 3), performance in this perceptual/iconic memory version of the task was perfect to near perfect in all participants (ranging between 95.3% and 100%).

In addition, we ran a surface-based morphometric analysis of the whole brain using the Qdec tool implemented in FreeSurfer to detect other possible cortical regions that might display a relationship between gray matter thickness and VWM (see Materials and Methods). In both hemispheres, the analysis revealed main clusters in the pericalcarine region where V1 is located. Among other smaller clusters, there were also main clusters in the paracentral region of the right hemisphere and in the rostral middle frontal region of the left hemisphere. However, none of these latter clusters survived corrections for multiple comparisons whereas those in the pericalcarine regions did, thereby supporting the notion of V1 being an important stage for setting individual differences in VWM (see Supplementary Table S1 and Fig. S2). Likewise, we computed additional cortical surface size analyses to examine the specificity of the relationship found between V1 surface size and VWM. To do so, we relied on cortical surface sizes as defined by the gyral-based Desikan–Killiany Atlas (Desikan et al. 2006) implemented in FreeSurfer. None of the sizes of these areas showed a significant relationship with VWM (all $P > 0.154$),

thereby supporting the notion that the relationship between surface size and VWM was exclusive to V1.

As our measures of V1 anatomy were derived from functional retinotopic mapping, we further examined whether the observed relationships would hold if V1 was defined anatomically (see Materials and Methods; Hinds et al. 2008). When V1 was defined anatomically, we again found a significant positive relationship between VWM and V1 volume ($r = 0.439$, $P = 0.014$). The relationship between V1 thickness and memory was also strong ($r = 0.696$, $P < 0.001$). In contrast, there was no significant relationship between the surface component of overall anatomical V1 and behavior ($r = 0.157$, $P = 0.400$), supporting the notion that the surface size of V1 representing central vision might be more important than the total V1 surface.

To further investigate the functional specificity of the observed brain–behavior relationship, we also tested a subsample ($N = 17$) of our participants using a numerical version of our visual working memory task, involving numbers instead of Gabor patterns. Using the same timing and spatial arrangement as in the VWM task, the numbers were presented in a circular array at the same eccentricity as the pattern stimuli in the VWM task. The split-half reliability of NWM showed intra-individual consistency (see Table 1 and Supplementary Results), and considerable inter-individual variability. In contrast to VWM and early visual cortex anatomy, we found no correlation between NWM and V1 gray matter volume ($r = 0.148$, $P = 0.571$; see Supplementary Fig. S3). An additional one-tailed Hotelling's T-test for the difference between the 2 correlational r values further confirmed the relationship between VWM and V1 volume to be to be significantly larger than the relationship between NWM and V1 volume ($t_{(14)} = 2.84$, $P = 0.007$). When looking at cortical thickness and surface size separately, results were similar (see Table 1, Supplementary Results and Fig. S4).

Discussion

Our findings indicate that the relationship between gray matter anatomy of primary visual cortex and VWM is functionally and structurally specific. Both V1 surface and thickness independently predicted performance in a VWM task. V1 was not linked to storage in non-visual spatial working memory measures, and VWM storage was not significantly related to the anatomy of any other brain area.

In the past, inter-individual variability in behavior, neural response, and anatomy has often been treated as "noise" and removed by averaging. However, inter-individual variability has recently been successfully exploited to uncover the mechanisms linking perception, cognition, and behavior to brain anatomy and function (Kanai and Rees 2011). Previous research has been able to link variability in V1 surface area to intra- and inter-individual differences in visual perception (Duncan and Boynton 2003; Schwarzkopf et al. 2011; Genç et al. 2014; Schwarzkopf and Rees 2013; Song et al. 2013). Our results extend these findings by showing that low-level sensory areas are not only a decisive stage for computing our present subjective experience of the world but also shape the way mental representations of the recent past are stored. This adds a new dimension to existing theories that limitations and individual differences in higher cognitive functions such as visual working memory might be mediated by the characteristics of the activity in high-level areas (Miller et al. 1996; Pessoa et al. 2002; Todd and Marois 2004, 2005; Vogel and Machizawa 2004; Xu and Chun 2005) and ties in well with the recently proposed model by Franconeri et al. (2013), which claims that individual memory items compete for space on anatomically delimited visual "maps," which, as we found, are larger in individuals with a higher visual working memory storage.

As the contrast of the Gabor patterns and the exposure duration of 1 s in the behavioral task ensured that perception was clearly in the suprathreshold zone, the risk that differences at the level of perceptual processing might have acted as a confounding factor in the observed relationships is very low and was excluded by a behavioral control experiment. In addition, perceptual orientation sensitivity thresholds, which have been linked to V1 structure (Song et al. 2013), occur within a much smaller range than the spatial orientation difference of 20° between our sample and test stimulus. We are therefore confident that the observed individual differences in our main condition are due to processes occurring during the retention phase, not the encoding phase.

Despite the finding that the amplitude of sustained activity in early visual cortex during visual working memory is low, it has been shown that sustained feature-selective activity patterns remain present (Harrison and Tong 2009; Serences et al. 2009; Riggall and Postle 2012; Emrich et al. 2013; Ester et al. 2013) and that transcranial magnetic stimulation of early visual cortex affects VWM performance both at the beginning and at the end of the retention phase (Cattaneo et al. 2009). The observed mnemonic activity patterns might be explained by recurrent local cortical networks (Wang 2001), whose localization in sensory areas has recently also been suggested by computational modeling approaches (Burak and Fiete 2012). According to these synaptic reverberation network models, sustained stimulus-selective activity patterns are maintained by excitatory and inhibitory connections.

It is possible that sustained orientation-selective activity patterns reach a higher fidelity and strength in individuals with a larger and/or thicker V1. Increases in cortical thickness have been attributed to a larger number of cells per column (Rakic 1988), greater neuronal arborization, size or number of neuroglia or regional vasculature (Zatorre et al. 2012; Carlo and Stevens 2013). Neuroglia are known to both coordinate and modulate neural signal transmission (Rusakov et al. 2011), and this ability might be increased with larger glial volume (Oberheim et al. 2012) and number. Importantly, recent research indicates that in the presence of larger glia far less stimulation is needed to boost or weaken the strength of synaptic transmission, both of which are essential for forming memory traces of sensory experiences (Han et al. 2013). Additionally, higher neuronal arborization could lead to a more finely woven network structure, thereby improving coordination and fine-tuning of neuronal interactions within the reverberatory network.

Regarding differences in surface size, it is known that neuron size does not scale proportionally with increases in surface size (Kaas 2000). This observation is compatible with the finding that early visual cortex surface size correlates positively with the number of neurons in these regions (Leuba and Garey 1987; Leuba and Kraftsik 1994). More neurons firing in response to a specific stimulus might in turn increase the likelihood that the strength of excitation surpasses a critical threshold necessary to generate a recurrent reverberatory state that persists when the stimulus is no longer present (Wang 2001).

In addition, surround suppression of individual items on a larger cortical V1 surface would overlap less, resulting in less inter-item competition and thus stronger representations of multiple items (Franconeri et al. 2013).

Interestingly, more recent studies also point at a potential link between GABA and V1 surface size. The concentration of this inhibitory neurotransmitter has been associated with the peak frequency of induced gamma oscillations in human visual cortex (Edden et al. 2009; Muthukumaraswamy et al. 2009; but see Cousijn et al. 2014). The peak of visually induced gamma oscillations has been shown to correlate positively with V1 surface area (Schwarzkopf et al. 2012). As recurrent inhibition has been suggested to ensure stimulus selectivity during mnemonic reverberation (Goldman-Rakic 1995), this mechanism should consequently be stronger with a higher presence of inhibitory circuits.

Independent of whether V1 was estimated anatomically or functionally, its volume and thickness predicted VWM performance. In the case of the surface component, however, we observed that only the area representing the more central portions of the visual field was predictive of behavioral performance. Hence, it might be more accurate to speak of a relationship with "V1 central cortical magnification" (Schwarzkopf and Rees 2013) rather than of a relationship with V1 surface *per se*. In addition, this finding might suggest that memory performance is best predicted by the size of the precise retinotopic V1 location where the stimuli are processed.

It is up to future work to examine how the anatomical properties of V1 might be linked to ERP components that predict individual memory performance (Vogel and Machizawa 2004). A link between these dynamic properties of the brain and the stable neuroanatomical features examined in our study might be particularly likely in light of a recent study, which established a link between individual V1 surface area and the amplitude of visually evoked potentials (Elvsåshagen et al. 2014). Another aspect requiring future investigation is whether the anatomical limitations of visual working memory are specific to the stimulus features, for example, complex stimuli like faces versus more simple stimuli like Gabor gratings. Such feature-specific anatomical correlates would be predicted by feature-specific "map" models of visual working memory (Franconeri et al. 2013).

Our findings might also have implications for potential links between the controversial topics concerning the efficacy of working memory training (Owen et al. 2010) and the degree of early visual cortex plasticity (Kirkwood et al. 1995; Wandell and Smirnakis 2009). Taken together, our results emphasize the importance of the basic anatomy of early sensory areas in acting as a bottleneck to our mental functioning, limiting the amount of information we can actively hold and manipulate in mind.

Supplementary Material

Supplementary material can be found at: http://www.cercor.oxfordjournals.org/.

Funding

This work was supported by Australian NHMRC project grants APP1024800 & APP1046198 and a Career Development Fellowship APP1049596 held by JP; JB was supported by an International Postgraduate Research Scholarship and a Brain Sciences UNSW PhD Top Up Scholarship.

Notes

We thank Luiz Lana for helpful discussions. *Conflict of Interest:* None declared.

References

Baddeley A. 2003. Working memory: looking back and looking forward. Nat Rev Neurosci. 4:829–839.
Brainard DH. 1996. The Psychophysics Toolbox. Spat Vis. 10:433–436.
Burak Y, Fiete IR. 2012. Fundamental limits on persistent activity in networks of noisy neurons. Proc Natl Acad Sci USA. 109: 17645–17650.
Carlo CN, Stevens CF. 2013. Structural uniformity of neocortex, revisited. Proc Natl Acad Sci USA. 110:1488–1493.
Cattaneo Z, Vecchi T, Pascual-Leone A, Silvanto J. 2009. Contrasting early visual cortical activation states causally involved in visual imagery and short-term memory. Eur J Neurosci. 30:1393–1400.
Cousijn H, Haegens S, Wallis G, Near J, Stokes MG, Harrison PJ, Nobre AC. 2014. Resting GABA and glutamate concentrations do not predict visual gamma frequency or amplitude. Proc Natl Acad Sci. 111(25):9301–9306.
Dale AM, Fischl B, Sereno MI. 1999. Cortical surface-based analysis I: segmentation and surface reconstruction. Neuroimage. 9:179–194.
Desikan RS, Ségonne F, Fischl B, Quinn BT, Dickerson BC, Blacker D, Buckner RL, Dale AM, Maguire RP, Hyman BT et al. 2006. An automated labeling system for subdividing the human cerebral cortex on MRI scans into gyral based regions of interest. Neuroimage. 31:968–980.
Duncan RO, Boynton GM. 2003. Cortical magnification within human primary visual cortex correlates with acuity thresholds. Neuron. 38:659–671.
Edden RAE, Muthukumaraswamy SD, Freeman TCA, Singh KD. 2009. Orientation discrimination performance is predicted by GABA concentration and gamma oscillation frequency in human primary visual cortex. J Neurosci. 29:15721–15726.
Elvsåshagen T, Moberget T, Bøen E, Hol PK, Malt UF, Andersson S, Westlye LT. 2014. The surface area of early visual cortex predicts the amplitude of the visual evoked potential. Brain Struct Funct. doi:10.1007/s00429-013-0703-7.
Emrich SM, Riggall AC, LaRocque JJ, Postle BR. 2013. Distributed patterns of activity in sensory cortex reflect the precision of multiple items maintained in visual short-term memory. J Neurosci. 33:6516–6523.
Ester EF, Anderson DE, Serences JT, Awh E. 2013. A neural measure of precision in visual working memory. J Cogn Neurosci. 25:754–761.
Filimonov I. 1932. Ueber die Variabilitaet der Grosshirnrindenstruktur. Mitt 2: regio occipitalis beim erwachsenen Menschen. J Psychol Neurol. 1–96.
Fischl B, Sereno MI, Dale AM. 1999. Cortical surface-based analysis II: inflation, flattening, and a surface-based coordinate system. Neuroimage. 9:195–207.
Fischl B, Sereno MI, Tootell RB, Dale AM. 1999. High-resolution intersubject averaging and a coordinate system for the cortical surface. Hum Brain Mapp. 8:272–284.
Franconeri SL, Alvarez GA, Cavanagh P. 2013. Flexible cognitive resources: competitive content maps for attention and memory. Trends Cogn Sci. 17:134–141.
Genç E, Bergmann J, Singer W, Kohler A. 2014. Surface area of early visual cortex predicts individual speed of traveling waves during binocular rivalry. Cereb Cortex. 34. doi:10.1093/cercor/bht342.
Goldman-Rakic PS. 1995. Cellular basis of working memory review. Neuron. 14:477–485.
Hagler DJ, Saygin AP, Sereno MI. 2006. Smoothing and cluster thresholding for cortical surface-based group analysis of fMRI data. Neuroimage. 33:1093–1103.

Han X, Chen M, Wang F, Windrem M, Wang S, Shanz S, Xu Q, Oberheim NA, Bekar L, Betstadt S et al. 2013. Forebrain engraftment by human glial progenitor cells enhances synaptic plasticity and learning in adult mice. Cell Stem Cell. 12:342–353.
Harrison SA, Tong F. 2009. Decoding reveals the contents of visual working memory in early visual areas. Nature. 458:632–635.
Hinds OP, Rajendran N, Polimeni JR, Augustinack JC, Wiggins G, Wald LL, Diana Rosas H, Potthast A, Schwartz EL, Fischl B. 2008. Accurate prediction of V1 location from cortical folds in a surface coordinate system. Neuroimage. 39:1585–1599.
Kaas J. 2000. Why is brain size so important: design problems and solutions as neocortex gets bigger or smaller. Brain Mind. 1:7–22.
Kanai R, Rees G. 2011. The structural basis of inter-individual differences in human behaviour and cognition. Nat Rev Neurosci. 12:231–242.
Kirkwood A, Lee H-K, Bear MF. 1995. Co-regulation of long-term potentiation and experience-dependent synaptic plasticity in visual cortex by age and experience. Nature. 375:328–331.
Kleiner M, Brainard D, Pelli D. 2007. What's new in Psychtoolbox-3? Perception, 36, ECVP Abstract Supplement, 14.
Leuba G, Garey L. 1987. Evolution of neuronal numerical density in the developing and aging human visual cortex. Hum Neurobiol. 6:11–18.
Leuba G, Kraftsik R. 1994. Changes in volume, surface estimate, three-dimensional shape and total number of neurons of the human primary visual midgestation until old age. Anat Embryol (Berl). 190:351–366.
Miller EK, Erickson CA, Desimone R. 1996. Neural mechanisms of visual working memory in prefrontal cortex of the macaque. J Neurosci. 16:5154–5167.
Muckli L, Kohler A, Kriegeskorte N, Singer W. 2005. Primary visual cortex activity along the apparent-motion trace reflects illusory perception. PLoS Biol. 3:e265.
Muthukumaraswamy SD, Edden RAE, Jones DK, Swettenham JB, Singh KD. 2009. Resting GABA concentration predicts peak gamma frequency and fMRI amplitude in response to visual stimulation in humans. Proc Natl Acad Sci USA. 106:8356–8361.
Oberheim NA, Goldman SA, Nedergaard M. 2012. Heterogeneity of astrocytic form and function. Methods Mol Biol. 814:23–45.
Owen AM, Hampshire A, Grahn JA, Stenton R, Dajani S, Burns AS, Howard RJ, Ballard CG. 2010. Putting brain training to the test. Nature. 465:775–778.
Panizzon MS, Fennema-Notestine C, Eyler LT, Jernigan TL, Prom-Wormley E, Neale M, Jacobson K, Lyons MJ, Grant MD, Franz CE et al. 2009. Distinct genetic influences on cortical surface area and cortical thickness. Cereb Cortex. 19:2728–2735.
Pelli DG. 1997. VideoToolbox software for visual psychophysics: transforming numbers into movies. Spat Vis. 10:437–442.
Pessoa L, Gutierrez E, Bandettini P, Ungerleider L. 2002. Neural correlates of visual working memory: fMRI amplitude predicts task performance. Neuron. 35:975–987.
Rakic P. 1988. Specification of cerebral cortical areas. Science (80-). 241:170–176.
Riggall AC, Postle BR. 2012. The relationship between working memory storage and elevated activity as measured with functional magnetic resonance imaging. J Neurosci. 32:12990–12998.
Rusakov DA, Zheng K, Henneberger C. 2011. Astrocytes as regulators of synaptic function: a quest for the Ca2+ master key. Neuroscientist. 17:513–523.
Schwarzkopf DS, Rees G. 2013. Subjective size perception depends on central visual cortical magnification in human V1. PLoS One. 8: e60550.
Schwarzkopf DS, Robertson DJ, Song C, Barnes GR, Rees G. 2012. The frequency of visually induced gamma-band oscillations depends on the size of early human visual cortex. J Neurosci. 32:1507–1512.
Schwarzkopf DS, Song C, Rees G. 2011. The surface area of human V1 predicts the subjective experience of object size. Nat Neurosci. 14:28–30.
Serences JT, Ester EF, Vogel EK, Awh E. 2009. Stimulus-specific delay activity in human primary visual cortex. Psychol Sci. 20:207–214.
Sereno AMI, Dale AM, Reppas JB, Kwong KK, Belliveau JW, Brady TJ, Rosen R, Tootell RBH. 1995. Borders of multiple visual areas in humans revealed by functional magnetic resonance imaging. Science (80-). 268:889–893.
Song C, Schwarzkopf DS, Rees G. 2013. Variability in visual cortex size reflects tradeoff between local orientation sensitivity and global orientation modulation. Nat Commun. 4:2201.
Stensaas SS, Eddington DK, Dobelle WH. 1974. The topography and variability of the primary visual cortex in man. J Neurosurg. 40:747–755.
Todd JJ, Marois R. 2004. Capacity limit of visual short-term memory in human posterior parietal cortex. Nature. 428:751–754.
Todd JJ, Marois R. 2005. Posterior parietal cortex activity predicts individual differences in visual short-term memory capacity. Cogn Affect Behav Neurosci. 5:144–155.
Vogel EK, Machizawa MG. 2004. Neural activity predicts individual differences in visual working memory capacity. Nature. 428:748–751.
Wandell BA, Dumoulin SO, Brewer AA. 2007. Visual field maps in human cortex. Neuron. 56:366–383.
Wandell BA, Smirnakis SM. 2009. Plasticity and stability of visual field maps in adult primary visual cortex. Nat Rev Neurosci. 10:873–884.
Wang XJ. 2001. Synaptic reverberation underlying mnemonic persistent activity. Trends Neurosci. 24:455–463.
Winkler AM, Kochunov P, Blangero J, Almasy L, Zilles K, Fox PT, Duggirala R, Glahn DC. 2010. Cortical thickness or grey matter volume? The importance of selecting the phenotype for imaging genetics studies. Neuroimage. 53:1135–1146.
Xing Y, Ledgeway T, McGraw PV, Schluppeck D. 2013. Decoding working memory of stimulus contrast in early visual cortex. J Neurosci. 33:10301–10311.
Xu Y, Chun MM. 2005. Dissociable neural mechanisms supporting visual short-term memory for objects. Nature. 440:91–95.
Zatorre RJ, Fields RD, Johansen-Berg H. 2012. Plasticity in gray and white: neuroimaging changes in brain structure during learning. Nat Neurosci. 15:528–536.